

## Observation of Magnetically Induced Effective-Mass Enhancement of Quasi-2D Excitons

L. V. Butov,<sup>1</sup> C. W. Lai,<sup>1,2</sup> D. S. Chemla,<sup>1,2</sup> Yu. E. Lozovik,<sup>3</sup> K. L. Campman,<sup>4</sup> and A. C. Gossard<sup>4</sup>

<sup>1</sup>Materials Sciences Division, E. O. Lawrence Berkeley National Laboratory, Berkeley, California 94720

<sup>2</sup>Department of Physics, University of California at Berkeley, Berkeley, California 94720

<sup>3</sup>Institute of Spectroscopy, Russian Academy of Sciences, 142092, Troitsk, Russia

<sup>4</sup>Department of Electrical and Computer Engineering, University of California, Santa Barbara, California 93106

(Received 7 May 2001; published 1 November 2001)

We present the first measurements of the dispersion relation of a quasi-2D magnetoexciton. We demonstrate that the magnetoexciton effective mass is determined by the coupling between the center-of-mass motion and internal structure and becomes overwhelmingly larger than the sum of the electron and hole masses in high magnetic fields.

DOI: 10.1103/PhysRevLett.87.216804

PACS numbers: 71.35.-y, 73.21.-b, 78.55.Cr

The physics of two dimensional (2D) systems of charged particles in a strong perpendicular magnetic field has attracted much attention over the last two decades. For example, single component 2D electron (or hole) gases exhibit the integer and fractional quantum Hall effects [1]. Two component 2D electron-hole neutral systems are also expected to possess curious properties at high magnetic fields. This is in particular the case of 2D excitons in perpendicular magnetic field (magnetoexcitons) whose composite  $e$ - $h$  structure has been predicted to result in intriguing effects [2]: (i) the 2D-magnetoexciton binding energy and effective mass are independent of the electron and hole effective masses and are determined by the magnetic field only [3,4]; (ii) although 2D magnetoexciton is a neutral particle, it reacts to the application of in-plane electric field as a single charge (Hall effect for exciton) [4,5]; (iii) in a direct band gap semiconductor the 2D-magnetoexciton ground state in in-plane electric field occurs at finite momentum [4–6].

The common origin of the aforementioned effects is that an exciton in a magnetic field exhibits a unique coupling between the internal structure and center-of-mass motion [7]. This coupling is a general property of elementary neutral excitations in a magnetic field. Along with interband magnetoexcitons this applies to the intraband excitations in 2DEG in quantizing magnetic fields: the spin-wave excitations [8–12], the magnetoplasmon excitations [8–11,13], and the quasiexcitons (a quasiexciton is a bound state of a quasiparticle and quasihole) in the fractional quantum Hall effect regime [9,11,12,14,15] described also as particle-hole pairs of composite fermions, called the CF excitons [16].

Figure 1 illustrates the physics behind that coupling for magnetoexcitons. The 2D magnetoexciton is made of an electron and a hole traveling with the same velocity,  $\mathbf{v}_g = \partial E_X / \partial \mathbf{P}$ , and producing on each other a Coulomb force which is exactly canceled by the Lorentz force [3,4] [ $\mathbf{P} \in \{\hat{x}, \hat{y}\}$  is the 2D-magnetoexciton center-of-mass momentum and  $E_X = E_X(\mathbf{P})$  is its dispersion law]. Applying this condition self-consistently determines  $E_X$  and, in turn, the binding energy  $E_B$  and the effective mass  $M_B$ . In

the high magnetic field limit, defined by the condition that  $E_B$  is much smaller than the  $e$  and  $h$  cyclotron energies, the problem can be solved analytically [3]: (i)  $E_B = \sqrt{\pi/2} e^2 / (\epsilon l_B) \sim \sqrt{B_\perp}$ , where  $l_B = \sqrt{\hbar c / (e B_\perp)}$  is the magnetic length and  $\epsilon$  is the dielectric constant, (ii)  $E_X(\mathbf{P}) = -E_B e^{-\beta} I_0(\beta)$ , where  $I_0(\beta)$  is modified Bessel function,  $\beta = [P l_B / (2\hbar)]^2$  [Fig. 1(c)], (iii) for  $P l_B / \hbar \ll 1$ ,  $M_B = (2^{3/2} \epsilon \hbar^2) / (\pi^{1/2} e^2 l_B) \sim \sqrt{B_\perp}$ , (iv) for magnetoexciton with  $P = 0$  the magnetic length plays the role of the Bohr radius, (v) magnetoexcitons with momentum  $\mathbf{P}$  carry an electric dipole in the direction perpendicular to  $\mathbf{P}$  whose magnitude,  $\langle \mathbf{r}_{eh} \rangle = \hat{z} \times \mathbf{P} l_B^2 / \hbar$ , is proportional to  $P$ . This expression makes explicit the coupling between the center-of-mass motion and the internal structure. The coupling results in a property, called the electrostatic analogy: the dispersion  $E_X(\mathbf{P})$  can be

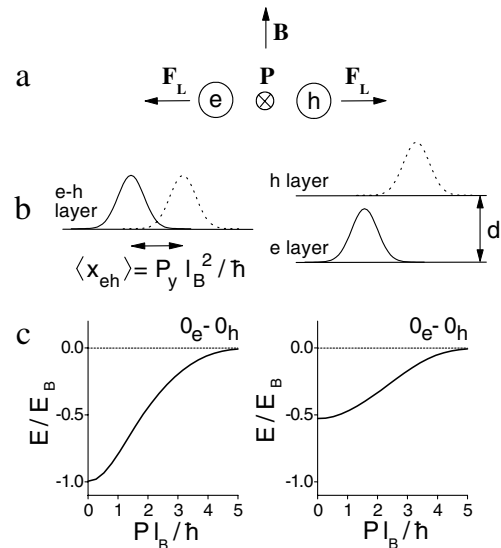


FIG. 1. Schematics showing (a) the coupling between the 2D-magnetoexciton center-of-mass and internal motions, (b) the separation between the electron and hole wave functions for 2D magnetoexciton (left) and quasi-2D indirect magnetoexciton (right). (c) Calculated dispersions of 2D magnetoexciton (left) and quasi-2D indirect magnetoexciton with  $d = l_B$  (right) in the high magnetic field limit.

calculated from the expression of the Coulomb force between the electron and the hole as a function of  $\langle \mathbf{r}_{eh} \rangle$  and has the unusual consequence that the magnetoexciton mass depends on the  $B_{\perp}$  only independent of the electron and hole masses. Contrary to the  $e$ - $h$  system at zero magnetic field (hydrogenic problem) all the  $e$ - $h$  pairs are bound states and there is no scattering state. At  $Pl_B/\hbar \gg 1$  the separation between electron and hole tends to infinity and the magnetoexciton energy evolves to the sum of the lowest  $e$  and  $h$  Landau level energies.

In this Letter we report the first measurement of a dispersion relation of quasi-2D magnetoexcitons. We find that the exciton effective mass is strongly enhanced as the perpendicular magnetic field increases and, at high fields, it becomes much larger than the sum of  $e$  and  $h$  masses. This experimental finding proves that a magnetoexciton is a quasiparticle whose effective mass is determined by the coupling between the center-of-mass motion and internal structure rather than by the masses of its constituents.

The principle of our experimental method is illustrated in Fig. 2. It is well known that the only free exciton states that can recombine radiatively are those inside the intersect between the dispersion surface  $E_X(\mathbf{P})$  and the photon cone  $E_{ph} = Pc/\sqrt{\epsilon}$  [17]. In GaAs structures the radiative zone corresponds to very small center-of-mass momenta  $K \leq K_0 \approx E_g\sqrt{\epsilon}/(\hbar c) \approx 2.7 \times 10^5 \text{ cm}^{-1}$ . Let us consider now a spatially indirect exciton with electron and hole confined in different layers parallel to the  $\{\hat{x}, \hat{y}\}$  plane.  $d$  is the distance between the layer centers. It has been shown in Refs. [18–20] that when a magnetic field  $B_{\parallel}$  is applied in the  $\{\hat{x}, \hat{y}\}$  plane the exciton dispersion surface shifts by  $P_B = -\frac{e}{c}dB_{\parallel}$  [Fig. 2(a)]. Therefore as  $B_{\parallel}$  increases the intersect of the photon cone with the exciton dispersion surface varies. Thus by measuring the dependence of the exciton photoluminescence (PL) energy as a function of the in-plane magnetic field  $B_{\parallel}$  one can determine the indirect exciton dispersion.

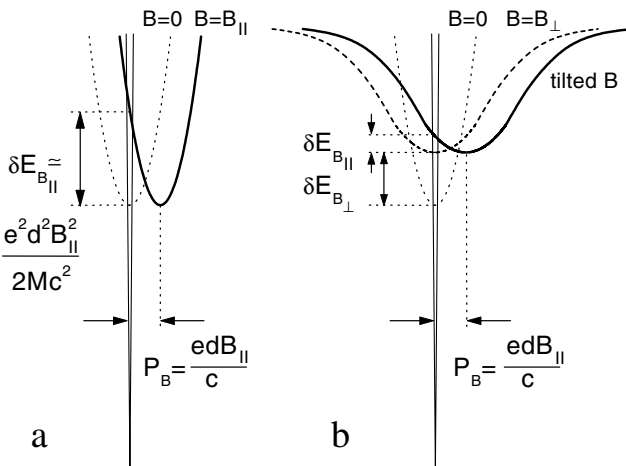


FIG. 2. Schematic of the indirect exciton dispersion (a) at zero and finite in-plane magnetic field  $B$  and (b) at zero  $B$ , perpendicular  $B$ , and tilted  $B$ . The optically active exciton states are within the radiative zone determined by the photon cone.

We use a  $n^+$ - $i$ - $n^+$  coupled quantum well (CQW) structure grown by molecular-beam epitaxy. The  $i$  region consists of two 8 nm GaAs QWs separated by a 4 nm  $\text{Al}_{0.33}\text{Ga}_{0.67}\text{As}$  barrier and surrounded by two 200 nm  $\text{Al}_{0.33}\text{Ga}_{0.67}\text{As}$  barrier layers. The  $n^+$  layers are Si-doped GaAs with  $n_{\text{Si}} = 5 \times 10^{17} \text{ cm}^{-3}$ . The separation of the  $e$  and  $h$  layers in the CQW (the indirect regime) is achieved by the gate voltage  $V_g$  applied between the  $n^+$  layers.  $V_g$  determines the external electric field in the  $\hat{z}$  direction  $F = V_g/d_0$ , where  $d_0$  is the  $i$ -layer width. The shift of the indirect exciton energy with increasing gate voltage  $\Delta E_{\text{PL}} = eFd$  allows the determination of the mean interlayer separation in the indirect regime  $d = 11.5 \text{ nm}$ , which is close to the distance between the QW centers. For the CQW studied the shift induced by strong in-plane magnetic fields  $K_B = \frac{e}{\hbar c}dB_{\parallel}$  is much larger than  $K_0$ . For example, at  $B_{\parallel} = 12 \text{ T}$ ,  $K_B \approx 2.1 \times 10^6 \text{ cm}^{-1} \sim 8 \times K_0$ . For the narrow QWs the diamagnetic shift of the bottom of the bands is very small and can be neglected [21], which is confirmed by the negligibly small energy shift of the spatially direct transitions (Fig. 3). Therefore, the peak energy of the indirect exciton PL is set by the energy of the radiative zone and is given as a function of  $B_{\parallel}$  by  $E_{p=0} = P_B^2/2M = e^2 d^2 B_{\parallel}^2 / (2Mc^2)$  for a parabolic dispersion, it is  $\propto 1/M$ . The PL measurements were performed in tilted magnetic fields  $\mathbf{B} = B_{\parallel}\hat{x} + B_{\perp}\hat{z}$  at  $T = 1.8 \text{ K}$  in a He cryostat with optical windows. The in-plane

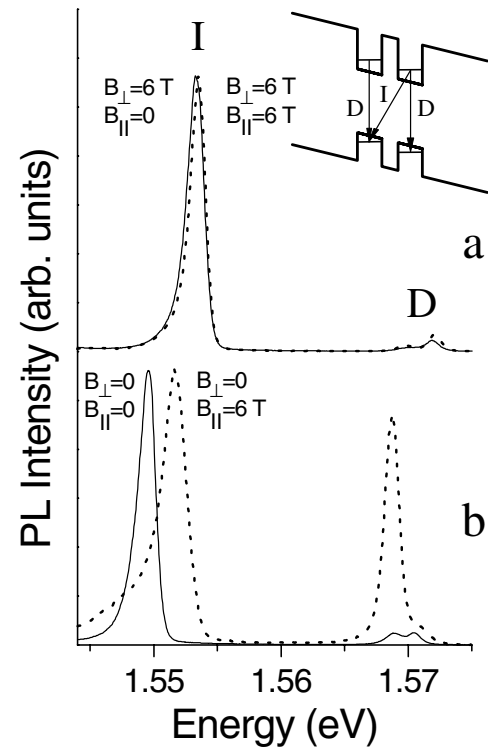


FIG. 3. PL spectra in magnetic fields  $\mathbf{B} = B_{\parallel}\hat{x} + B_{\perp}\hat{z}$  for different perpendicular,  $B_{\perp}$ , and parallel,  $B_{\parallel}$ , components at  $V_g = 1 \text{ V}$ . The intensities are normalized. Inset: Schematic of the band diagram of the GaAs/ $\text{Al}_x\text{Ga}_{1-x}\text{As}$  CQW.

component of  $\mathbf{B}$  was used to measure the dispersion of the magnetoexciton (Fig. 2). Carriers were photoexcited by a HeNe laser at an excitation density  $0.1 \text{ W/cm}^2$ .

The basic features of the indirect magnetoexciton are the same as that of the direct magnetoexciton. They are also determined by the coupling between the magnetoexciton internal structure and center-of-mass motion [Fig. 1(b), right and Fig. 1(c), right]. However, because of the separation between the electron and hole layers the indirect magnetoexciton binding energy and effective mass differ quantitatively from those of direct magnetoexciton. As  $d$  increases the indirect magnetoexciton binding energy reduces whereas its effective mass increases. In particular, for  $d \ll l_B$ ,  $M_{Bd} = M_B[1 + 2^{3/2}d/(\pi^{1/2}l_B)]$  and for  $d \gg l_B$ ,  $M_{Bd} = M_B\pi^{1/2}d^3/(2^{3/2}l_B^3)$  [22]. The mass enhancement is explained using the electrostatic analogy: for separated layers the  $e$ - $h$  Coulomb interaction is weaker than that within a single layer and changes only slightly for  $\langle \mathbf{r}_{eh} \rangle \lesssim d$ ; this implies that  $E_X(P)$  increases only slowly for  $P \lesssim \hbar d/l_B^2$ ; in other words, the indirect magnetoexcitons have a large effective mass.

The spatially direct transitions ( $D$ ) and the indirect transition ( $I$ ) seen in Fig. 3 are identified by the PL kinetics and  $V_g$  dependence. The direct PL lines have short decay time and their positions practically do not depend on  $V_g$ , while the indirect exciton PL line has long decay time and shifts to lower energies with increasing  $V_g$  [23].

As  $B_{\parallel}$  increases the energy of indirect (magneto)exciton increases (Fig. 3) due to the displacement of the dispersion surface in momentum space, while the energies of the direct transitions are practically unchanged. The magnitude of the PL energy shift is smaller for the higher  $B_{\perp}$  [compare Figs. 3(a) and 3(b)]. The PL line shift vs  $B_{\parallel}$  determines the magnetoexciton dispersion. This is presented in Fig. 4(a) for various  $B_{\perp}$ . The magnetoexciton effective mass at the band bottom is determined by the quadratic fits to the dispersion curves at small  $K$ . At  $B_{\perp} = 0$  the measured PL energy shift rate corresponds to  $M = 0.22m_0$ . This value is in good agreement with the calculated mass of heavy hole exciton in GaAs QWs  $\approx 0.25m_0$  (electron mass  $m_e = 0.067m_0$  and in-plane heavy hole mass  $m_h = 0.18m_0$ ; see, e.g., Ref. [24]). Drastic changes of the magnetoexciton dispersion are observed at finite  $B_{\perp}$ . The dispersion curves become significantly flat at small momenta as seen in Fig. 4. This corresponds to a strong enhancement of the magnetoexciton mass: already at  $B_{\perp} = 4 \text{ T}$  the magnetoexciton mass has increased by about 3 times and at higher  $B_{\perp}$  the dispersions become so flat that the scattering of the experimental points does not allow precise determination of that mass which becomes very large.

The experimental results are now compared with *ab initio* calculations. The Hamiltonian is

$$\hat{H} = \frac{1}{2m_e} \left( i \frac{\partial}{\partial \mathbf{r}_e} - \frac{e}{c} \mathbf{A}(\mathbf{r}_e, z_e) \right)^2 + \frac{1}{2m_h} \left( -i \frac{\partial}{\partial \mathbf{r}_h} + \frac{e}{c} \mathbf{A}(\mathbf{r}_h, z_h) \right)^2 + V(r), \quad (1)$$

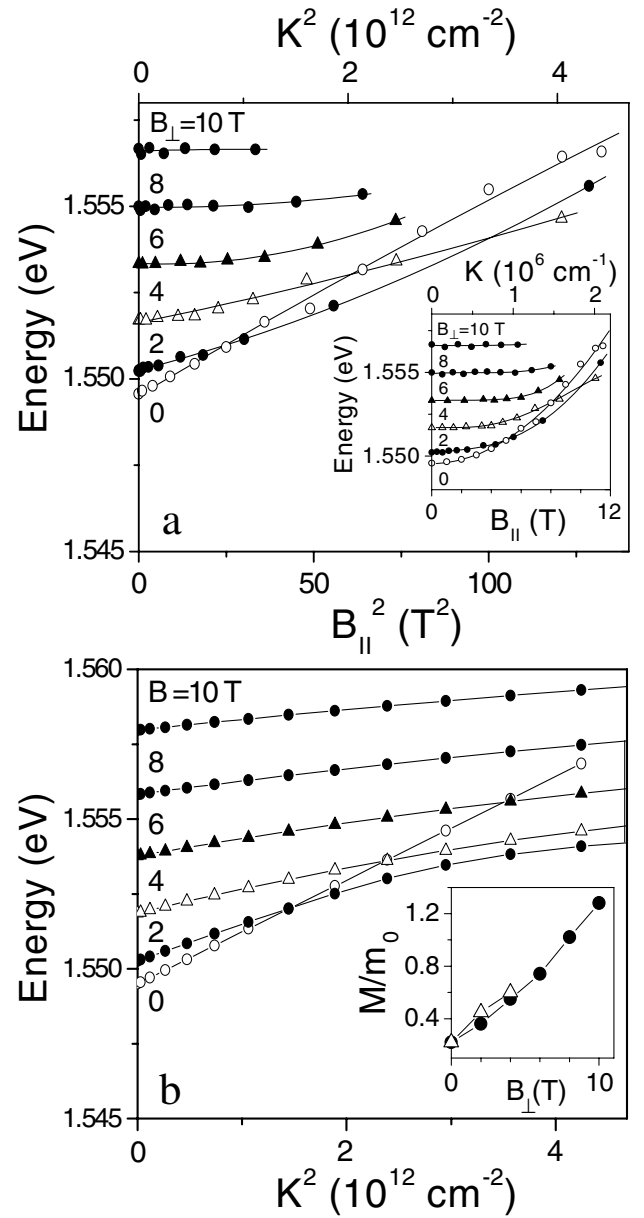


FIG. 4. (a) Measured and (b) calculated magnetoexciton dispersions at  $B_{\perp} = 0, 2, 4, 6, 8,$  and  $10 \text{ T}$  vs  $K^2$ . Upper inset: Measured magnetoexciton dispersions vs  $K$  ( $B_{\parallel}$ ). Lower inset: Measured (triangles) and calculated (circles) magnetoexciton mass at the band bottom vs  $B_{\perp}$ .

where  $\mathbf{r}_e$  and  $\mathbf{r}_h \in \{\hat{x}, \hat{y}\}$  are the in-plane  $e$  and  $h$  radii vectors,  $\mathbf{r} = \mathbf{r}_e - \mathbf{r}_h$ ,  $\mathbf{R} = [m_e\mathbf{r}_e + m_h\mathbf{r}_h]/M$ , and  $V(r) = -\frac{1}{\epsilon\sqrt{d^2+r^2}}$  is  $e$ - $h$  interaction. The magnetic moment  $\mathbf{P}$  is conserved because of the translation invariance along the  $\{\hat{x}, \hat{y}\}$  plane and gauge invariance. Using the gauge  $\mathbf{A}(\mathbf{r}) = \frac{1}{2}\mathbf{B}_{\perp} \times \mathbf{r} + \hat{x}B_y z - \hat{y}B_x z$ , we have  $\mathbf{P} = -i\frac{\partial}{\partial \mathbf{R}} + \frac{e}{2c}\mathbf{B}_{\perp} \times \mathbf{r} + \frac{e}{c}\mathbf{B}_{\parallel} \times d\hat{z}$  [3,7]. Therefore, in the two-layer model  $\mathbf{B}_{\parallel}$  causes only a shift of the magnetic moment and a displacement of the magnetoexciton dispersion  $E_X(\mathbf{P})$  by  $\frac{e}{c}\mathbf{B}_{\parallel} \times d\hat{z}$ , similar to the  $B_{\perp} = 0$  case [18–20]. For the magnetoexciton in perpendicular field  $\mathbf{B} = \mathbf{B}_{\perp}$  after a gauge transformation

$\Psi_{\mathbf{P}}(\mathbf{R}, \mathbf{r}) = \exp(-i\frac{e}{2c}\mathbf{B}_{\perp} \times \mathbf{R} \cdot \mathbf{r})\psi_{\mathbf{P}}(\mathbf{R}, \mathbf{r})$  the Hamiltonian takes the form

$$\hat{H} = \frac{1}{2M} \left( \frac{\mu}{\kappa} \right)^2 \mathbf{P}^2 + \frac{1}{2\mu} \left( i \frac{\partial}{\partial \mathbf{r}} \right)^2 + \frac{eB_{\perp}}{2c\kappa} \hat{L}_z + \frac{1}{2\mu} \left( \frac{eB_{\perp}}{2c} \mathbf{r} - \frac{2\mu}{M} \hat{z} \times \mathbf{P} \right)^2 + V(r), \quad (2)$$

where  $\hat{L}_z$  is the angular momentum operator along  $\hat{z}$  and the last two terms represent, respectively, the interaction with the magnetic field and the Coulomb interaction,  $\mu^{-1} = m_e^{-1} + m_h^{-1}$ ,  $\kappa^{-1} = m_e^{-1} - m_h^{-1}$ .

The calculations of magnetoexciton dispersion (Fig. 4) are performed using the imaginary time approach and the direct descent technique for a time-dependent Schrödinger equation with Hamiltonian given by Eq. (2). We find that in a finite magnetic field the effective mass which characterizes the dispersion at small  $P$  monotonically grows with  $B_{\perp}$ . The calculated effective mass enhancement is in excellent, better than 10%, agreement with the experimental data [25]; e.g., at  $B_{\perp} = 4$  T the measured magnetoexciton mass increase is 2.7 as compared to the current theoretical 2.5; see Fig. 4. The agreement still remains qualitatively good at high momenta (e.g., both experiment and theory show that at high  $P$  the magnetoexciton dispersions at finite  $B_{\perp}$  become lower in energy than the exciton dispersion at  $B_{\perp} = 0$ ); however, the theory gives a rate of energy increase with momentum at high  $P$  slower than the experiment. This quantitative difference could be accounted for by including details such as the effects of the finite QW thickness and finite radiative zone width (note also that the experimental accuracy for the line position decreases at the highest  $B_{\parallel} \gtrsim 10$  T, i.e., for the largest momenta  $P/\hbar \gtrsim 1.8 \times 10^6$  cm $^{-1}$ , due to the line broadening and strong intensity reduction).

The observed large enhancement of the effective mass of the indirect exciton in magnetic fields is a single-exciton effect contrary to the well known renormalization effects in neutral and charged  $e$ - $h$  plasmas [26]. It has, however, very important effects on collective phenomena in the exciton system. In particular, the mass enhancement explains the disappearance of the stimulated exciton scattering and the transition from the highly degenerate to classical exciton gas with increasing magnetic field observed in Ref. [27].

This work was supported by the Director, Office of Energy Research, Office of Basic Energy Sciences, Division of Material Sciences of the U.S. Department of Energy, under Contract No. DE-AC03-76SF00098 and by RFBR and INTAS grants.

[1] For recent reviews, see *Perspectives in Quantum Hall Effects*, edited by S. Das Sarma and A. Pinczuk (Wiley, New

- York, 1997); H.L. Stormer, D.C. Tsui, and A.C. Gossard, *Rev. Mod. Phys.* **71**, S298 (1999).
- [2] We consider here *single* 2D-magnetoexciton effects only. Besides this, we focus only on 2D-magnetoexciton buildup from electron and hole at the 0th Landau levels.
- [3] I.V. Lerner and Yu.E. Lozovik, *Zh. Eksp. Teor. Fiz.* **78**, 1167 (1980) [*Sov. Phys. JETP* **51**, 588 (1980)].
- [4] D. Paquet, T.M. Rice, and K. Ueda, *Phys. Rev. B* **32**, 5208 (1985).
- [5] A.B. Dzyubenko and Yu.E. Lozovik, *Fiz. Tverd. Tela (Leningrad)* **26**, 1540 (1984) [*Sov. Phys. Solid State* **26**, 938 (1984)].
- [6] A. Imamoglu, *Phys. Rev. B* **54**, R14 285 (1996).
- [7] L.P. Gor'kov and I.E. Dzyaloshinskii, *Zh. Eksp. Teor. Fiz.* **53**, 717 (1967) [*Sov. Phys. JETP* **26**, 449 (1968)].
- [8] Yu.A. Bychkov, S.V. Iordanskii, and G.M. Eliashberg, *Pis'ma Zh. Eksp. Teor. Fiz.* **33**, 152 (1981) [*JETP Lett.* **33**, 143 (1981)].
- [9] C. Kallin and B.I. Halperin, *Phys. Rev. B* **30**, 5655 (1984).
- [10] A. Pinczuk, J.P. Valladares, D. Heiman, A.C. Gossard, J.H. English, C.W. Tu, L. Pfeiffer, and K. West, *Phys. Rev. Lett.* **61**, 2701 (1988).
- [11] A. Pinczuk, B.S. Dennis, L.N. Pfeiffer, and K. West, *Phys. Rev. Lett.* **70**, 3983 (1993).
- [12] H.D.M. Davies, J.C. Harris, J.F. Ryan, and A.J. Turberfield, *Phys. Rev. Lett.* **78**, 4095 (1997).
- [13] A.H. MacDonald, H.C.A. Oji, and S.M. Girvin, *Phys. Rev. Lett.* **55**, 2208 (1985).
- [14] F.D.M. Haldane and E.H. Rezayi, *Phys. Rev. Lett.* **54**, 237 (1985).
- [15] S.M. Girvin, A.H. MacDonald, and P.M. Platzman, *Phys. Rev. Lett.* **54**, 581 (1985).
- [16] R.K. Kamilla, X.G. Wu, and J.K. Jain, *Phys. Rev. Lett.* **76**, 1332 (1996).
- [17] J. Feldmann, G. Peter, E.O. Göbel, P. Dawson, K. Moore, C. Foxon, and R.J. Elliott, *Phys. Rev. Lett.* **59**, 2337 (1987).
- [18] A.A. Gorbatsevich and I.V. Tokatly, *Semicond. Sci. Technol.* **13**, 288 (1998).
- [19] L.V. Butov, A.V. Mintsev, Yu.E. Lozovik, K.L. Campman, and A.C. Gossard, *Phys. Rev. B* **62**, 1548 (2000).
- [20] A. Parlange, P.C.M. Christianen, J.C. Maan, I.V. Tokatly, C.B. Soerensen, and P.E. Lindelof, *Phys. Rev. B* **62**, 15 323 (2000).
- [21] F. Stern, *Phys. Rev. Lett.* **21**, 1687 (1968).
- [22] Yu.E. Lozovik and A.M. Ruvinskii, *Zh. Eksp. Teor. Fiz.* **112**, 1791 (1997) [*Sov. Phys. JETP* **85**, 979 (1997)].
- [23] L.V. Butov, A.A. Shashkin, V.T. Dolgoplov, K.L. Campman, and A.C. Gossard, *Phys. Rev. B* **60**, 8753 (1999).
- [24] G.E.W. Bauer and T. Ando, *Phys. Rev. B* **38**, 6015 (1988); B.R. Salmassi and G.E.W. Bauer, *ibid.* **39**, 1970 (1989).
- [25] The only fitting parameter in the calculations is  $M_X$  at  $B_{\perp} = 0$  which was obtained separately from the measured exciton dispersion at  $B_{\perp} = 0$ :  $M_X = 0.22m_0$ .
- [26] S. Schmitt-Rink, D.S. Chemla, and D.A.B. Miller, *Adv. Phys.* **38**, 89 (1989).
- [27] L.V. Butov, A.I. Ivanov, A. Imamoglu, P.B. Littlewood, A.A. Shashkin, V.T. Dolgoplov, K.L. Campman, and A.C. Gossard, *Phys. Rev. Lett.* **86**, 5608 (2001).